Journal of Crystal Growth 54 (1981) 507–518
North-Holland Publishing Company

THE GROWTH OF METASTABLE, HETEROEPITAXIAL FILMS OF α-Sn BY METAL BEAM EPITAXY

R.F.C. FARROW, D.S. ROBERTSON, G.M. WILLIAMS, A.G. CULLIS, G.R. JONES, I.M. YOUNG and P.N.J. DENNIS

Royal Signals and Radar Establishment, St. Andrews Road, Malvern, Worcs. WR14 3PS, UK

Received 30 January 1981

Heteroepitaxial films of α-Sn have been prepared for the first time. The films were grown in an MBE system by direct condensation of a beam of Sn atoms onto clean, ordered (001) surfaces of InSb and CdTe held at $T \sim 25°C$. In-situ RHEED studies indicate that the films grow by a two-dimensional layer mechanism with a (2 × 2) surface reconstruction throughout growth. Above a film thickness of ~0.5 μm nucleation and growth of β-Sn occurred. α-Sn films of ≲0.5 μm in thickness are a substrate-stabilized metastable phase which undergoes a reversible $\alpha \rightarrow \beta$ phase transformation at ~70°C. The presence of uniaxial strain in the films has been confirmed by double-crystal X-ray diffraction measurements which reveal that the films have tetragonal symmetry as a result of in-plane compression imposed by the constraint of epitaxy. Ge-doping of the α-Sn films permits growth of films thicker than 0.5 μm and reduces the degree of uniaxial strain.

1. Introduction

It is well known (Busch and Kern [1]) that the element Sn can undergo a phase transformation from its usual metallic (β) phase to a lower temperature (α) phase ("grey" tin) which has the diamond structure. The discovery in 1950 (Busch and Kern [1]) of the semiconducting properties of α-Sn stimulated many attempts at preparation of single crystal samples. Although bulk crystals of α-Sn were prepared by Ewald and Tufte [2] all attempts at growth of single crystal films (Becker [3]) were reported as unsuccessful. However, with the great improvements in vacuum technology over the past decade and the development of the technique of metal beam epitaxy (Farrow et al. [4–7]) for the preparation of epitaxial films of metals on semiconductors, it seemed logical to the authors to attempt heteroepitaxy of α-Sn (a = 6.489 Å at 25°C) on the isomorphous, closely lattice matched crystals InSb (a = 6.4798 Å at 25°C) and CdTe (a = 6.4829 Å at 25°C) under clean, controlled conditions. The success of this approach is described in this paper.

2. Experimental techniques

The heteroepitaxial films α-Sn were prepared in an ion and titanium sublimation pumped molecular beam epitaxy similar to that described earlier for the preparation of epitaxial InP (Farrow [8]) and metal films (Farrow et al. [5]). The techniques of Auger electron spectroscopy (AES) and reflection high energy electron diffraction (RHEED) were used to characterise the surfaces of the InSb and CdTe substrates prior to growth and the α-Sn films after growth. The Sn beam source was a Knudsen effusion oven constructed (Farrow and Williams [6]) of high purity pyrolytic boron nitride and tantalum radiation shields. An isothermal double oven containing separated charges of Sn and Ge was used to provide the 1% Ge in Sn beam used in growing Ge stabilized α-Sn films. The Sn charge for the Knudsen effusion oven was taken from a double zone refined Sn ingot of purity >99.999%. The Ge charge was from a single crystal Ge boule of resistivity ~100 ΩM, purity >99.999%. Modulated beam mass spectrometry was used to monitor the intensity and composition of beams impinging on the substrate. During film growth the residual background pressure was $<5 \times 10^{-9}$ Torr. The CdTe(001) orientation wafers (resistivity $>10^8$

0022-0248/81/0000–0000/$02.50

Ω cm) were polished by combined chemical and mechanical action using 2% Br in methanol as the etchant. The InSb(001) orientation wafers (n-type, $n_D - n_A \sim 10^{14}$ cm^{-3}, $\mu \sim 5 \times 10^5$ cm^2 V^{-1} s^{-1} at 77 K) were mechanically polished using diamond paste and subsequently subjected to a free etch in a proprietry oxidising solution by the manufacturers (MCP Electronic Materials Ltd). Immediately prior to loading the wafers were rinsed in hot iso-propyl alcohol. Selected area deposition of Sn, when required, was achieved by interposing a molybdenum mask between beam source and substrate.

X-ray texture analysis of the Sn films was carried out using a cylindrical texture camera of the type described by Wallace and Ward [9]. Lattice parameter measurements of the α-Sn films were made by double crystal diffractometry using the technique described by Bartels and Nijman [10], and an automated APEX diffractometer equipped with a second axis [11,12]. Both scanning and transmission electron microscopy were carried out in a JEM 120C microscope. In some cases, Sn was deposited onto prethinned discs of InSb to facilitate subsequent transmission observations.

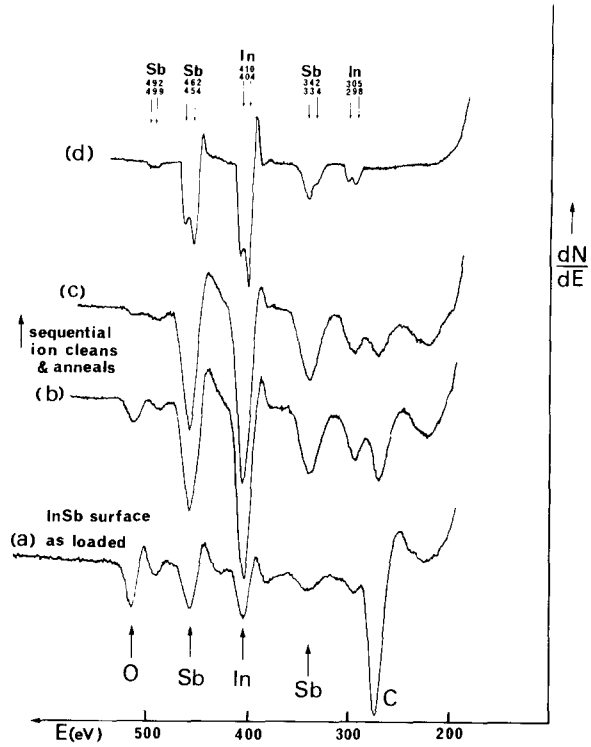

Fig. 1. Auger spectra of InSb(001) surface recorded before and at various stages of surface preparation prior to heteroepitaxial growth of α-Sn: (a) as loaded; (b) after 500 eV Ar^+ ion bombardment at 1.5 μA cm^{-2} for 1 h followed by a 1 h anneal at $T = 200$°C; (c) after a further cycle of the above treatment; (d) after a third cycle of the treatment, spectrum recorded at higher resolution than (a)–(c).

3. Substrate preparation and film growth

Auger spectra of the InSb and CdTe substrate surfaces prior to in-situ cleaning always showed considerable C and O surface contamination. This is illustrated in the case of InSb by fig. 1a. Low (500 eV) energy argon ion bombardment at a current density of 1.5 μA cm^{-2} followed by annealing at 200°C was found to be the most reproducible way of achieving well ordered, impurity free surfaces which sustained reproducible epitaxial α-Sn films. Figs. 1b–1d show Auger spectra of InSb(001) which illustrate the sequential removal of O and C by this process. The spectrum in fig. 1d was recorded after an integrated dose of ~10^{17} (Ar^+ 500 eV) ions cm^{-2} and an integrated anneal time of 3 h. The O and C impurities have been reduced below the detection limit of ~1% monolayer. Side effects of ion bombardment such as In metal island formation (Cullis and Farrow [13]) were found to be negligible at the ion dose levels ($\lesssim 10^{17}$ cm^{-2}) used in this work.

Reflection electron diffraction patterns of the InSb(001) surface (see fig. 2) recorded along [110] and [1$\bar{1}$0] azimuths after sample cleaning and annealing indicated (2 × 4) surface reconstruction whilst for CdTe only bulk diffraction streaks were observed in both azimuths indicating (1 × 1) surface symmetry.

Following substrate preparation the Sn oven temperature was adjusted to give an arrival rate of Sn atoms equivalent to a growth rate of 0.5 μm h^{-1} and the substrate temperature to −20°C. Film growth was then commenced by opening the Sn oven shutter. The electron diffraction pattern changed to (2 × 2) symmetry immediately growth commenced (see fig. 2c) and remained with this symmetry up to an α-Sn film thickness of ≃0.5 μm. No change in the spacing of the bulk diffraction streaks was observed during

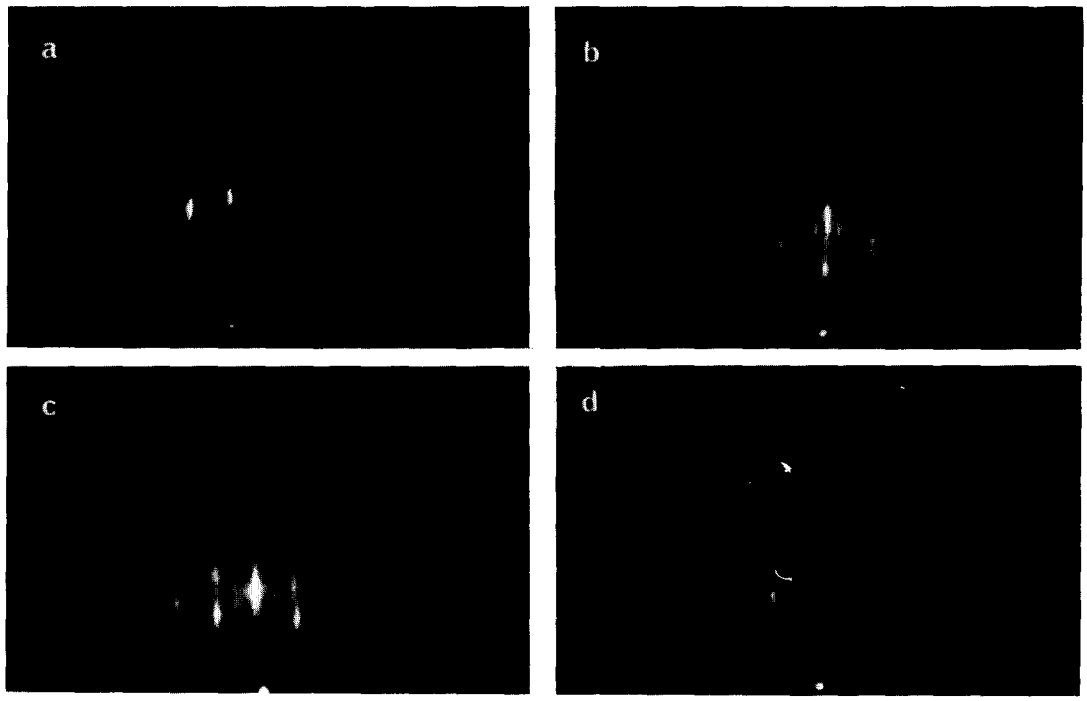

Fig. 2. Reflection electron diffraction patterns recorded before and after α-Sn growth on InSb(001), electron energy 5 keV, beam current 1 μA: (a) InSb(001) surface immediately prior to α-Sn growth, beam along [110] azimuth; (b) InSb(001) surface immediately prior to α-Sn growth, beam along [1$\bar{1}$0] azimuth; (c) after growth of 0.1 μm α-Sn, beam along [110] azimuth; (d) after growth of 0.5 μm α-Sn, beam along [110] azimuth.

growth up to 0.5 μm, indicating that the film consisted of α-Sn not β-Sn which has a considerable lattice mismatch to both InSb and CdTe. During growth, the substrate temperature increased to +25°C as a result of radiation heating from the Knudsen oven ($T \simeq 1270$°C). As the film thickness was increased beyond 0.5 μm the diffraction streaks became more diffuse with evidence of a departure from cubic symmetry. β-Sn nucleii became visible as white specks on an otherwise mirror-smooth reflecting film. X-ray texture analysis on films thicker than 0.5 μm confirmed (see section 4) the white specks as β-Sn regions. Ge-doped α-Sn films were prepared from a beam of composition 1% Ge in Sn. In the case of these films no significant change in the quality of the (2 × 2) symmetry α-Sn diffraction pattern was observed as the film increased in thickness beyond 0.5 μm. Moreover, the film remained mirror smooth and reflecting.

4. Structural analysis of the films

The structure and surface morphology of the α-Sn films were examined by scanning and transmission electron microscopy, electron channeling, X-ray texture analysis and X-ray diffractometry. In particular, the microscopy studies of the films showed directly the dynamics of the phase transformation.

4.1. Electron microscope studies of α-Sn films: as-deposited and during transformation

When relatively thin (~2000 Å) as-grown α-Sn films on (001)InSb substrates were examined in the scanning electron microscope (SEM) they were found to be relatively uniform with only slight background undulations on the scale of ~200 Å. However, some discontinuities on the scale of ~1000 Å were also present, as shown in fig. 3a. These may have been

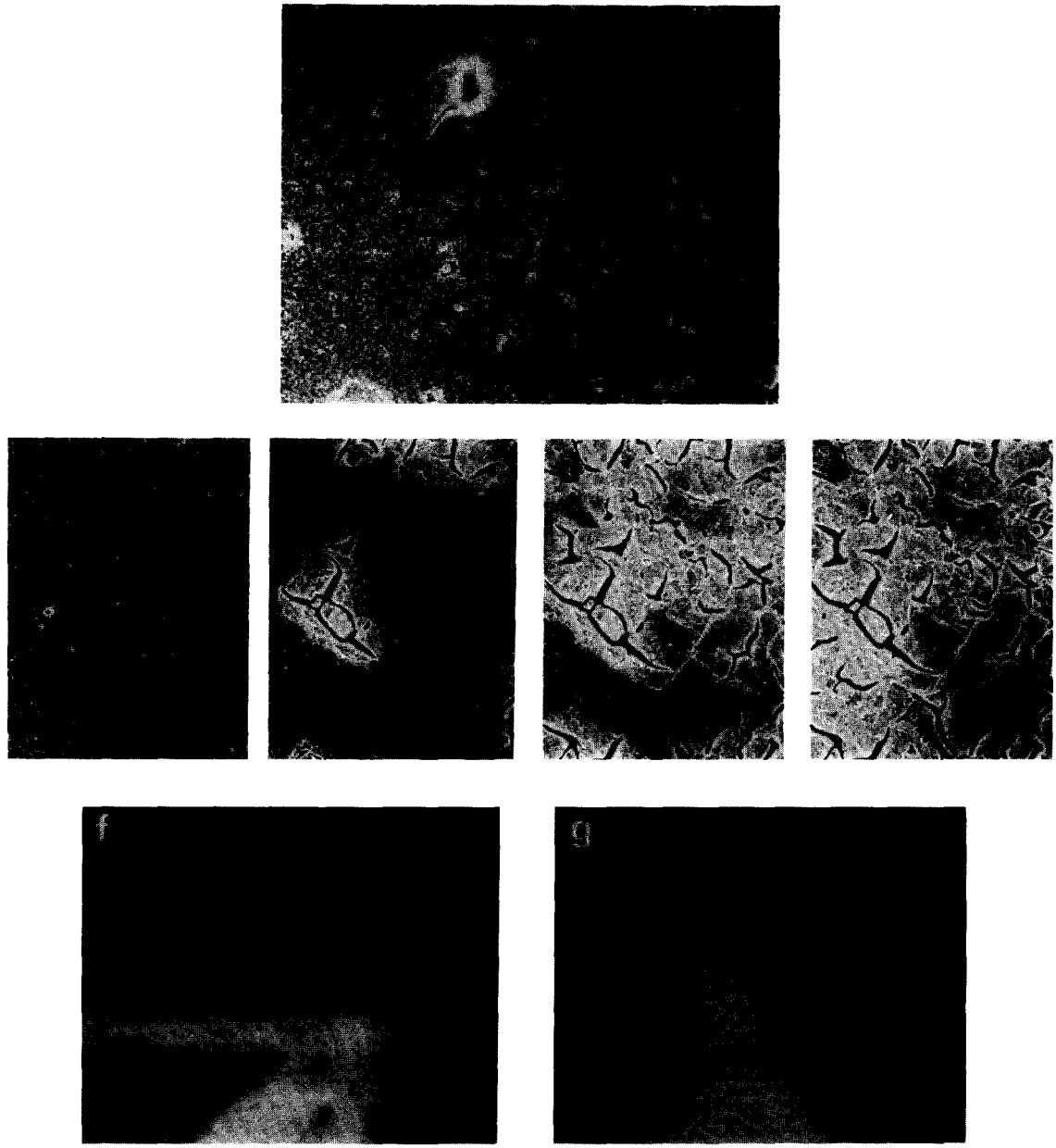

Fig. 3. Scanning secondary electron micrographs of a Sn film on (001)InSb: (a), (b) as-deposited; (c), (d), (e) during progressive α to β transformation at ~75°C. Electron channelling patterns (f), (g) correspond to the as-deposited and transformed phases, respectively.

produced by deposition of Sn onto substrate surface irregularities. Nevertheless, the overall good uniformity of the film is demonstrated in fig. 3b and, indeed, electron channelling patterns confirmed (fig. 3f) that is orientation was (001), matching that of the substrate. When this film was heated in the SEM hot-stage it was possible to directly observe the details of the α-Sn to β-Sn transformation. For tem-

peratures up to 60°C there was little evidence of change in the film structure. However, when the temperature was raised to ~75°C the β-Sn phase was seen to nucleate in local areas which then expanded into the remaining α-Sn film. This process is illustrated in figs. 3c–3e where the newly forming β-Sn appears brighter than the original film and contains microcracks due to its increased density. Within a period of approximately 15 min the transformation to β-Sn was complete and electron channelling patterns (fig. 3g) showed few features indicating that the film crystal perfection had been severely degraded.

It is interesting to note that, when a film transformed as described above was cooled towards room temperature, partial reformation of the original α-Sn phase was observed. However, after a further heating cycle at 75°C to reconvert the Sn to the β-phase, the reformation of α-Sn could not be achieved by cooling.

Prethinned discs of InSb onto which ~200 Å thick Sn films had been deposited were examined in the transmission electron microscope (TEM). This study confirmed that the initial α-Sn overgrowth was perfectly aligned with the (001)InSb substrate (fig. 4a), the film itself containing few extended crystallographic defects. However, a scattered distribution of small inclusions was observed and, when the specimen was heated to ~75°C in the TEM hot stage, islands of β-Sn were often seen to nucleate and grow at these locations (fig. 4b). The interphase boundaries were sometimes locally straight, and as shown in fig. 4c the transformed β-phase material was polycrystalline in nature. Further details will be given elsewhere (Cullis and Farrow [14]).

4.2. X-ray analysis of as-grown α-Sn films

X-ray texture patterns of Sn films up to 0.5 μm thick grown on clean, ordered InSb and CdTe substrates showed only one set of diffraction spots (see fig. 5a) consistent with parallel epitaxy of α-Sn. The lattice parameter mismatch between the α-Sn film and InSb or CdTe substrates is <0.2% which resulted in indistinguishable Bragg diffractions on the texture pattern. Double crystal X-ray diffraction was used to deconvolute the substrate and film diffractions (see below). X-ray texture patterns recorded from 0.2 μm thick Sn films deposited onto O and C contaminated substrates which had not been subjected to ion cleaning and annealing showed (see fig. 5b) the presence of lines due to polycrystalline β-Sn. β-Sn lines were also observed from Sn films, thicker than 0.5 μm grown onto clean, annealed substrates. However, in the case of films doped with 1% Ge, the texture pattern showed only a single set of diffraction spots, indicating parallel epitaxy of α-Sn, even for films as thick as 1 μm. In addition, β-Sn lines were observed from Sn films deposited onto ion cleaned substrates

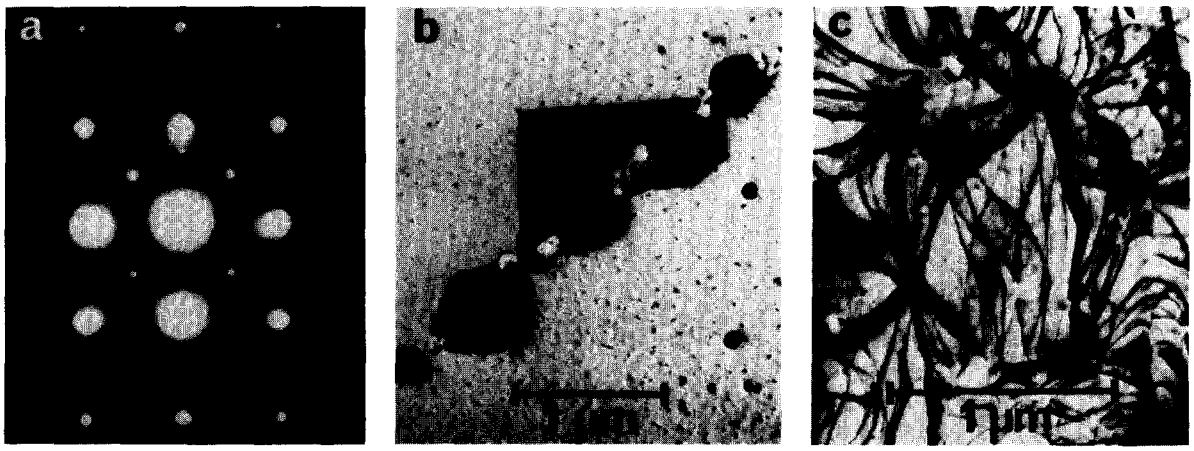

Fig. 4. Transmission electron diffraction pattern (a) corresponds to as-deposited (001)α-Sn on (001)InSb. Transmission images (b), (c) show the formation and growth of the polycrystalline β phase.

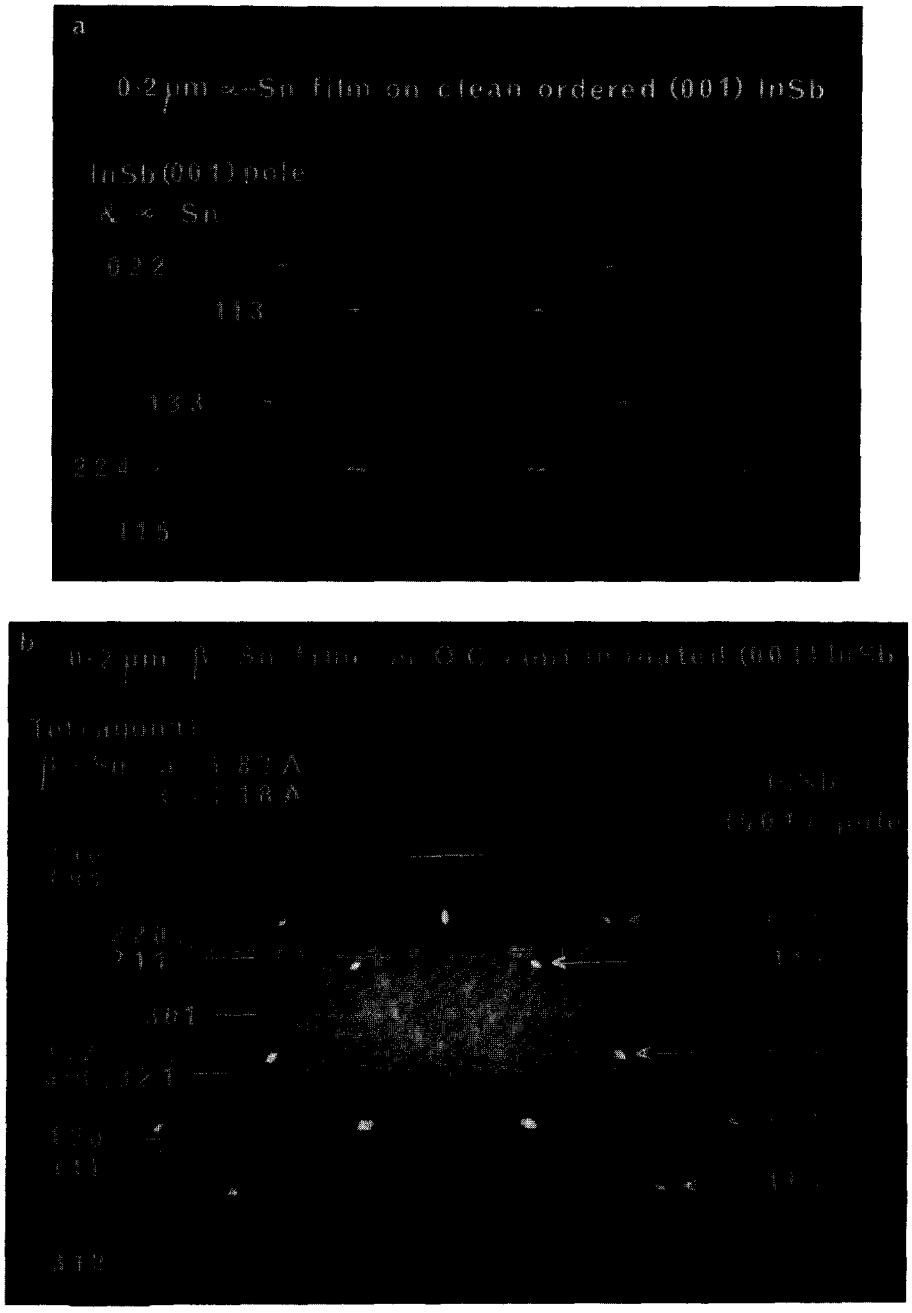

Fig. 5. (a) X-ray texture pattern of 0.2 μm thick α-Sn film grown in a clean, ordered InSb(001) substrate. The single set of diffraction spots is consistent with parallel epitaxy of α-Sn. CrKα radiation. (b) X-ray texture pattern of 0.2 μm thick β-Sn film on O, C contaminated region of InSb(001) substrate. In this case the polycrystalline nature of the β-Sn film is evident from the horizontal (constant θ) powder lines all of which can be attributed to tetragonal β-Sn. CrKα radiation.

which had not been annealed to restore surface order. These observations show that for nucleation and growth of α-Sn it is necessary for the substrates to be both clean and ordered.

Double crystal X-ray diffraction measurements were made on α-Sn films grown onto both CdTe and InSb (001) orientation substrates and on 1% Ge-doped α-Sn films on InSb. Double crystal rocking curves for these three cases are shown in fig. 6 and the state of strain of the epitaxial layers is detailed in table 1. Data were derived from diffraction experiments using different X-ray wavelengths which are given under the "*hkl*" entry where Cr, Fe and Cu refer to chromium, iron and copper Kα, radiation, ϕ is the inclination of the lattice planes with the crystal surface. θ (deg) is the calculated Bragg angle from

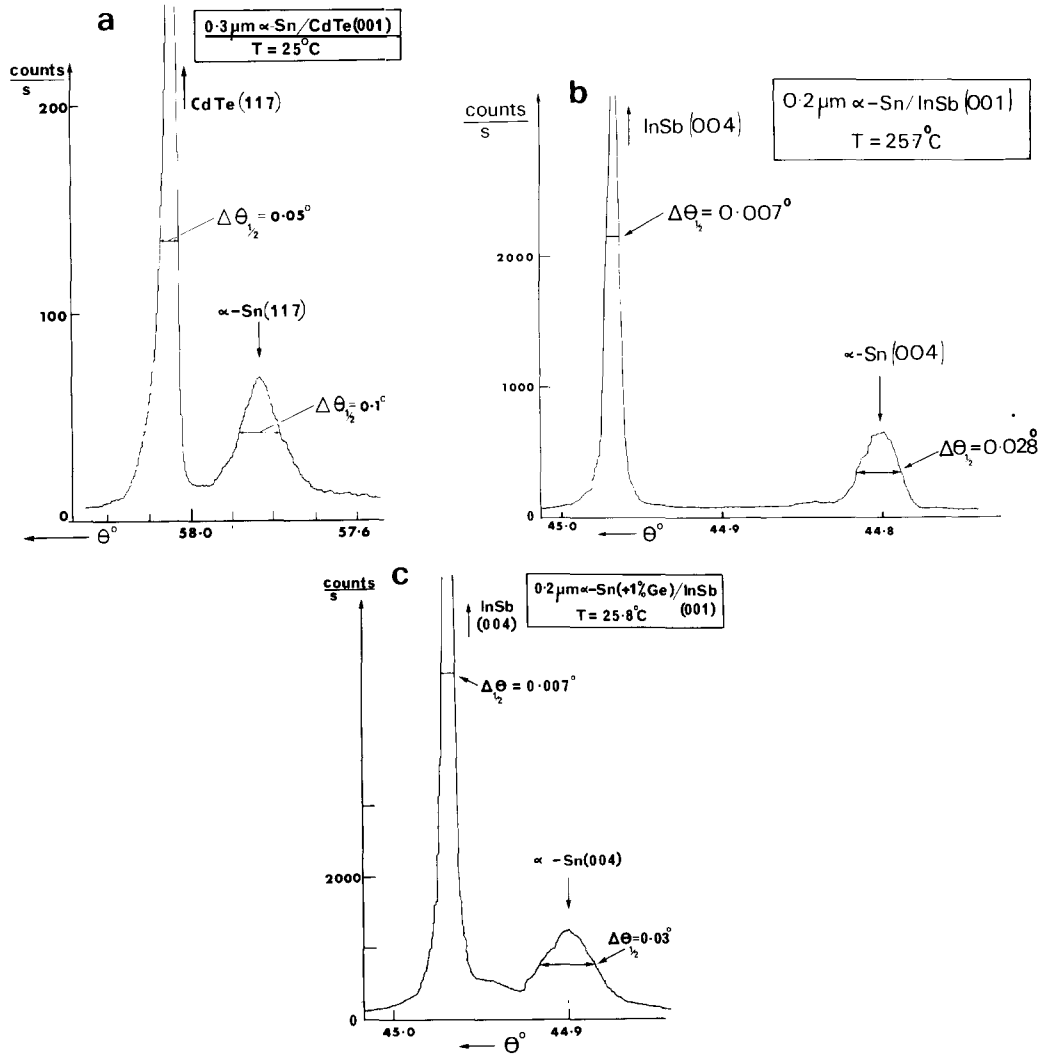

Fig. 6. (a) Double crystal rocking curve for 0.2 μm thick film of α-Sn on (001)CdTe; CuKα radiation, T = 25°C. Analysing crystal: gadolinium gallium garnet (888) Bragg diffraction. (b) Double crystal rocking curve for 0.2 μm thick film of α-Sn on (001)InSb; CrKα radiation, T = 25.7°C (004)α-Sn/InSb with analysing crystal silicon (113). (c) Double crystal rocking curve for 0.2 μm thick film of 1% Ge-doped α-Sn on (001)InSb; CrKα radiation. T = 25.8°C. (004)α-Sn/InSb with analysing crystal silicon (113). $\Delta\theta\frac{1}{2}$ refers to full width (in degrees) at half maximum peak height.

Table 1
Lattice parameter data for α-Sn films, determined by double crystal X-ray diffraction (for details of the table see text)

hkl	ϕ (deg)	θ (deg)	$\Delta\theta$ (s)	$(\Delta d/d)_{obs}$ $\times 10^4$	$(\Delta d/d)_{calc}$ $\times 10^4$	Substrate lattice parameter at 25°C (Å)
α-Sn on InSb(001):						
004 Cr	0	44.97	558(13)	27.1(6)		
004 Fe	0	36.70	419(9)	27.3(5)		
008 Cu	0	71.99	1710(17)	27.0(2)		
117 Cu	11.3	58.10	894(17)	27.0(5)	26.1	6.47980(1)
115 Cr	15.6	66.64	1243(17)	26.0(4)	25.1	
115 Fe	14.6	50.92	669(13)	26.3(5)	25.1	
224 Cr	35.3	59.94	619(15)	17.4(4)	18.0	
α-Sn (1% Ge) on InSb(001):						
004 Cr	0	44.97	237(8)	11.5(4)		
117 Cu	11.3	58.10	373(13)	11.2(4)	11.1	6.47980(1)
115 Cr	15.6	66.64	486(13)	10.2(3)	10.7	
224 Cr	35.3	59.94	227(9)	7.8(3)	7.7	
α-Sn on CdTe(001):						
004 Cr	0	44.94	415(25)	20.2(12)		6.48289(1)
224 Cr	35.3	59.90	501(25)	14.1(7)	13.5	

the substrate lattice parameter measured by the Bond method [15]. Differentiation of Bragg's Law yields

$$\Delta d/d = \Delta\theta \cot\theta ,$$

where $\Delta d/d = (d_L - d_S)/d_S$, and d_L and d_S refer to the lattice parameters of the layer and substrate respectively. $\Delta\theta$ (s) is derived from the double-crystal experiment using the peak separation of the substrate and layer. $(\Delta d/d)_{calc}$ was computed from the relationship $(\Delta d/d)_\perp \cos^2\phi$, where $(\Delta d/d)_\perp$ is the measured difference in the lattice plane spacing perpendicular to the growth direction. In all cases the width of the film diffraction peaks is greater than that of the substrate. This may indicate a higher density of structural defects in the film than in the substrate, although diffraction broadening effects due to the rather thin layers (0.2 μm) cannot be excluded. The width of the CdTe substrate diffraction peaks is considerably greater than that of InSb which is due largely to the presence of low angle grain boundaries in the CdTe crystals used in the study [16]. The diffraction conditions used in recording the rocking curves in figs. 6b and 6c were identical and it is concluded from the smaller separation of the substrate and film peaks in the latter case, that the addition of 1% Ge to the Sn brings the α-Sn lattice parameter closer to the value for the InSb substrate. The values of $(\Delta d/d)$ calculated from $(\Delta d/d)_\perp \cos^2\phi$ are in good agreement with the observed values, and are consistent with a symmetrical uniaxial strain in the α-Sn films. In all three cases there is lattice matching at the interface by an in-plane compression of the film. This results in an elastic distortion and dilation of the film along [001], giving a tetragonal symmetry. Using the approach of Hornstra and Bartels [17], a value for the unstrained α-Sn lattice parameter has been estimated from the relationship

$$(\Delta a/a)_{relax} = (\Delta d/d)_\perp (1 - \nu)/(1 + \nu) ,$$

where ν is the Poisson ratio. If a magnitude of 0.57 is assumed for $(1 - \nu)/(1 + \nu)$, which is the value for Si and Ge, then $a_{relax} = 6.4897(2)$ Å is derived for undoped α-Sn. This is close to the literature value of 6.489 for α-Sn [18]. A similar calculation for Ge doped α-Sn yields 6.4839(2) Å for the unstrained lattice parameter. The addition of Ge significantly reduces the mismatch and the uniaxial strain as expected, on the assumption that Vegard's Law holds for solid solutions of Ge in α-Sn. From values of the unstrained lattice parameter for α-Sn (derived above)

and a literature value of 5.6576 Å for Ge [19], the level of Ge in the α-Sn film is calculated to be 0.7%. The calculated Ge level is close to that expected (~1%) from a consideration of the vapour pressure of Ge, the temperature of the Knudsen effusion oven and the expected unity sticking coefficient for Ge.

4.3. X-ray analysis of the effect of heating on the Ge-doped α-Sn films

An X-ray diffraction analysis was made of the effect of increased temperature on a 1 μm thick, 1% Ge-doped α-Sn film. Electron channelling studies mentioned previously of undoped α-Sn films showed that the $\alpha \rightarrow \beta$ transformation occurred at ~70°C and was reversible for a single transformation cycle. The integrated diffractions from the (200), (101) and (211) peaks of the tetragonal symmetry β-Sn phase were monitored as a function of sample temperature at 10°C intervals. Fig. 7 shows the results of the measurements. It is clear that the onset of the $\alpha \rightarrow \beta$ transformation is in the temperature range 70–80°C. This is in agreement with the finding of Ewald [20] that addition of 0.75 wt% Ge to Sn increased the $\alpha \rightarrow \beta$ transformation temperature to at least 60°C. It is interesting that, unlike the undoped Sn films, the transformation of the Ge-doped film was irreversible on cooling to 20°C.

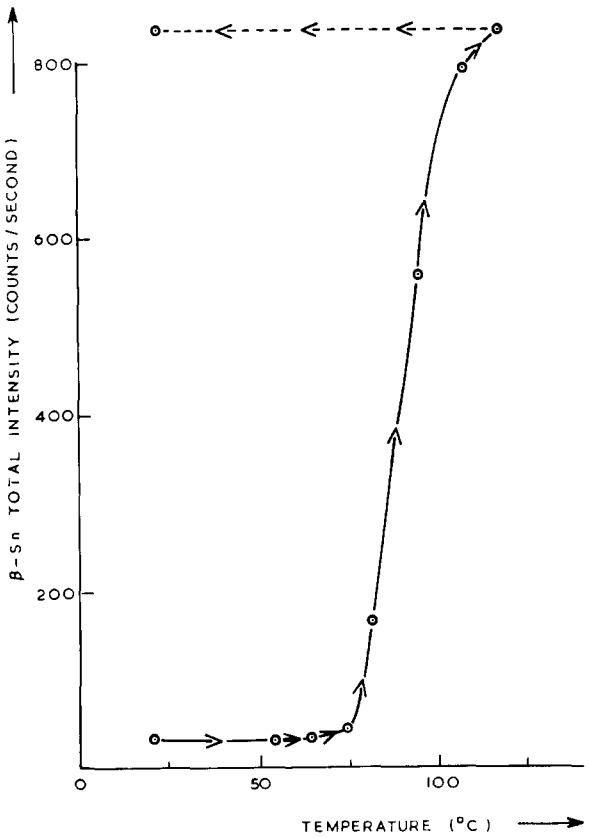

Fig. 7. Integrated intensity of (200), (101) and (211) Bragg peaks from the tetragonal β-Sn phase present in a 1% Ge-doped α-Sn film as a function of temperature. The curve represents the $\alpha \rightarrow \beta$ phase transformation in the film. The small but significant initial count rate at 20°C is partly due to background counts and partly to a localized β-Sn region present in the sample area analysed.

5. Electrical measurements

Hall mobility measurements were carried out on 0.5 μm thick α-Sn films grown on high resistivity (>10^6 Ω) CdTe(001) orientation substrates. These

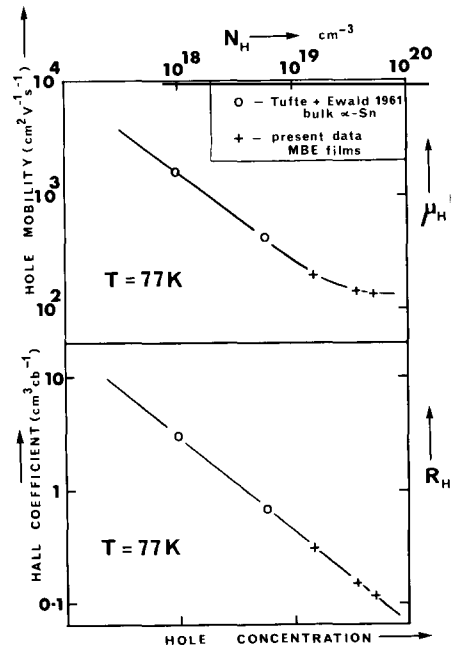

Fig. 8. 77 K hole mobility (μ_H) and Hall coefficient (R_H) as a function of hole concentration: (○) bulk samples of α-Sn, data from Tufte and Ewald [21]; (+) present data, MBE grown films.

measurements showed that the films were reproducibly p-type with carrier concentrations in the range $(1-4)\times10^{19}$ cm^{-3} at 77 K and 77 K hole mobilities in the range 100–250 cm^2 V^{-1} s^{-1}. The mobilities and Hall coefficients for three representative films are plotted as a function of carrier concentration in fig. 8. Data for p-type α-Sn single crystal samples reported by Tufte and Ewald [21] are also plotted in fig. 8. The μ_H and R_H values for the films lie on lines of smooth extrapolation from the data of Tufte and Ewald for p-type crystals of α-Sn grown from mercury solution. Initial measurements for 1% Ge-doped α-Sn films indicate similar carrier concentrations and mobilities to those shown in fig. 8.

D.C. $I-V$ measurements for p-type α-Sn/n-type InSb heterojunctions recorded at 77 K showed the expected rectifying diode characteristic. Values of zero bias resistance (R_0)–junction area (A) products were in the range $R_0A \sim 1-10\ \Omega$ cm^2. Infra-red photovoltaic response measurements for these diodes confirmed a significant response at wavelengths greater than the InSb cut off at 5.7 μm. Initial measurements suggest an optical band gap for the α-Sn of ~0.12 eV.

6. Discussion

The successful growth of heteroepitaxial films of α-Sn described in this paper may be contrasted with the earlier unsuccessful attempts (Becker [3]) in which growth was attempted on InSb, Ge and other substrates in an oil diffusion pumped bell jar evaporator system. In the latter case the residual background pressure was ~10^{-5} Torr with H_2O, CO, CO_2 and hydrocarbons as the main vapour species. This would have rendered impossible the removal of contaminant impurity atoms, such as C and O, from the substrate surface prior to growth. Thus, as we have shown, only the β-Sn phase would have grown under such conditions. Clearly, for α-Sn film growth, Sn atom condensation must occur on a clean and well ordered isomorphous substrate.

The RHEED observation of a strongly streaked (2 × 2) pattern during the initial stage of film growth, and subsequently, supports the view that the α-Sn grows by a two-dimensional layer mechanism rather than by nucleation and coalescence of metal islands as observed by the author and co-workers (Farrow et al. [4–7], Cullis and Farrow [13]) in the cases of epitaxy of Ag, Al and Au on InP substrates prepared in the same way as the InSb substrates in this work. This view is supported by the investigations of the α-Sn films described in section 4.1.

The stability of the epitaxial α-Sn films to ~70°C and the reversibility of the $\alpha \rightarrow \beta$ transformation at temperatures well above the generally accepted bulk transformation temperature of 13.2°C are both confirmation that the films are a substrate-stabilized metastable phase. The entire interface acts as a seed crystal for the α-phase since the absence of surface impurities ensures intimate epitaxial contact between substrate and film. Clearly the interface has a lower misfit energy (Van der Merwe [23]) than the substrate/β-Sn interface which would have to accommodate a considerable mismatch in symmetry and dimension probably via a high density of interfacial dislocations.

The lattice parameter measurements show that the substrate/α-Sn misfit is accommodated largely by misfit elastic strain which leads to the tetragonal distortion of the α-Sn lattice discussed in section 4.1. With increasing film thickness during growth the influence of the substrate on newly condensing Sn atoms will diminish and a point will eventually be reached at which nucleation of β-Sn during growth at $T >$ 13.2°C will become as likely as continued growth of α-Sn. This limiting thickness appears to be ≃0.5 μm.

Ge-doping was found to have the same stabilizing influence on the α-Sn phase as that reported by Ewald [20]. Unlike the introduction of Ge into α-Sn from solution in liquid Sn, however, there should be no limitation to the levels of Ge and Si which may be introduced into the α-Sn by the method described in this paper.

Electrically, the two most significant findings are that the films are strongly p-type and that the p–n heterojunction photodiodes exhibit significant photovoltaic response beyond the InSb long wavelength cut-off of 5.7 μm at 77 K. Since the Sn source material used in the Knudsen oven contains $<10^{16}$ cm^{-3} total impurity atoms it may be excluded as the origin of $>10^{19}$ cm^{-3} acceptor impurities in the film. However, three other possible causes should be considered. Firstly, at the Sn oven operating temperature of 1270°C significant thermal decomposition

of the pyrolytic boron nitride components of the oven is expected on thermodynamic grounds. For example, the dissociation vapour pressure of N_2 over boron nitride at 1270°C, calculated using ΔH° and S° values from the National Bureau of Standards compilation [22], is $p(N_2) \simeq 10^{-5}$ Torr. This would correspond to an impurity level of 0.1% in the Sn beam but since the sticking coefficient of N_2 under MBE conditions is expected to be zero (N_2 is a volatile gas at the MBE growth temperature of ~25°C) no resultant electrical effects on the film are to be expected. On the other hand, the solid boron product of the oven dissociation is expected to have a significant vapour pressure of monatomic boron at 1270°C. Data on p(B) over boron cover a very wide range. For example, p(B) at 1270°C calculated from ref. [22] is 3.4×10^{-9} Torr. However, Knudsen effusion data on carefully outgassed crystalline boron summarized by Nesmeyanov [28] give $p(B) = 10^{-3}$ Torr. This latter level would correspond to an impurity level of 10% in the Sn beam! Modulated beam mass spectrometric (MBMS) studies showed no evidence for boron at this level. However, since the MBMS detection limit in this work was rather high it is possible that boron at the 0.1% level could have been present. Assuming the sticking cpefficient of boron (a likely acceptor impurity in α-Sn) to be unity, under the present α-Sn growth conditions, such a level could account for the measured acceptor concentration of $\sim 10^{19}$ cm^{-3}. Secondary ion mass spectrometry (SIMS) studies have in fact confirmed boron as the main film impurity and therefore qualitatively support the view that oven dissociation is the cause of p-type doping.

Two other causes of spurious dopings are possible, however, and cannot be excluded at this stage. These are the autodoping of the film by outdiffusion of substrate elements and the possible electrical activity of point defects in the films. It is well known (Montgomery et al. [24]) that the deposition of metal films on compound semiconductors, such as GaAs, InP or CdTe can result in displacement of substrate atoms which may migrate to the surface of the metal film during deposition. In-situ Auger analysis during the present experiments show no evidence of this effect but it is possible that In or Cd (from InSb or CdTe substrates could be uniformly distributed through the α-Sn films at a level of $\sim 10^{19}$ cm^{-3} (i.e. ~0.05%) which is below the detection limit of the present Auger system. SIMS analyses of the films do not support this model. As for the possibility of electrically active point defects being responsible for the p-type electrical activity, it is conceivable that some localized nucleation of β-Sn could result in vacancies or vacancy–metal complexes in the α-Sn lattice which may have associated acceptor levels. Whilst some localized β-Sn regions do occur at regions of disturbance at the film–substrate interface (see section 4.1) the bulk is free of β-Sn nucleii and it seems unlikely at this stage that native defects are responsible for the p-type doping of the films.

The presence of uniaxial stress in the films is likely to have a profound influence on the band structure of α-Sn. Assuming the band structure model of Groves and Paul [25] holds for bulk α-Sn, dilation of the α-Sn lattice in the [001] direction is expected (Averous [26]) to lead to overlapping of the Γ_8 heavy and light hole bands and thus to an increasing degree of metallic behaviour. On the other hand a compressive strain along [001] is expected to lead to a separation of the Γ_8 bands, thus opening up a gap and converting α-Sn from a semimetal to a semiconductor. This model, however, appears to be at variance with the measured structural and electrical properties of the present films. For example, the measured uniaxial dilation along [001] for α-Sn on InSb is equivalent to [001] uniaxial tension which according to Averous would lead to metallic behaviour rather than the semiconducting behaviour indicated by the Hall data and photovoltaic response measurements. The effect of differential thermal expansion of Sn and InSb (Novikova [27]) is such that only a small reduction in uniaxial strain is expected on cooling from 300 to 77 K. Certainly, an inversion in the sign of the strain can be excluded on the basis of Novikova's data. Clearly, measurements on the shape of the optical absorption edge and photoconductivity of higher purity films are required to clearly resolve the band structure of α-Sn.

7. Conclusions

Heteroepitaxial α-Sn films have been grown on clean, ordered (001) InSb and CdTe surfaces under controlled and monitored conditions in an MBE sys-

tem. The structural and electrical properties of these films have been explored and the main conclusion may be summarized as follows:

(1) Heteroepitaxial α-Sn films, up to 0.5 μm thick, grow readily on clean, ordered (001) InSb and (001) CdTe surfaces at $T \sim 25°C$ by direct condensation of a beam of Sn atoms.

(2) A necessary condition for α-Sn growth is that the substrate surface be both clean and ordered. This was achieved in the present experiments by low-energy ion bombardment and annealing. Deposition of Sn on surfaces with O or C as impurities or residual disorder resulted in nucleation and growth of β-Sn.

(3) The α-Sn films are a substrate-stabilized metastable phase which undergoes a reversible $\alpha \rightarrow \beta$ phase transformation at ~70°C. Ge-doping of the α-Sn films permits growth of films thicker than 0.5 μm by increasing the bulk transformation temperature to ~70°C.

(4) The α-Sn films are strongly p-type, probably as a result of boron doping arising from the dissociation of the boron nitride oven components.

(5) The presence of uniaxial strain in the α-Sn films has been confirmed by double crystal X-ray diffraction measurements. These measurements have revealed that the film has tetragonal symmetry as a result of in-plane compression imposed by the constraint of epitaxy.

Acknowledgements

The authors are grateful to R.G. Humphreys for pointing out the influence of uniaxial strain on the band structure of α-Sn, and to D.T.J. Hurle for helpful discussions and encouragement throughout the work. The assistance of N. Chew in TEM sample preparation is also gratefully acknowledged. Thanks are also due to Brian Bellamy of UK AEA Harwell for the X-ray diffraction studies of the alpha to beta transformation.

References

[1] G.A. Busch and R. Kern, Solid State Phys. 11 (1961) 1.
[2] A.W. Ewald and O.N. Tufle, J. Appl. Phys. 29 (1958) 1007.
[3] J.H. Becker, J. Appl. Phys. 29 (1958) 1110.
[4] R.F.C. Farrow, J. Phys. D. (Appl. Phys.) 10 (1977) L135.
[5] R.F.C. Farrow, A.G. Cullis, A.J. Grant and J.E. Pattison, J. Crystal Growth 45 (1978) 292.
[6] R.F.C. Farrow and G.M. Williams, Thin Solid Films 55 (1978) 303.
[7] R.F.C. Farrow, A.G. Cullis, A.J. Grant, G.R. Jones and R. Clampitt, Thin Solid Films 58 (1979) 189.
[8] R.F.C. Farrow, in: Crystal Growth and Materials, Eds. E. Kaldis and H.J. Scheel (North-Holland, Amsterdam, 1977) ch. I.7.
[9] C.A. Wallace and R.C.C. Ward, J. Appl. Cryst. 8 (1975) 42.
[10] W.J. Bartels and W. Nijman, J. Crystal Growth 44 (1978) 518.
[11] M. Hart and K.H. Lloyd, J. Appl. Cryst. 8 (1975) 42.
[12] G.R. Jones, K.H. Lloyd and I.M. Young, to be published.
[13] A.G. Cullis and R.F.C. Farrow, Thin Solid Films 58 (1979) 197.
[14] A.G. Cullis and R.F.C. Farrow, to be published.
[15] W.L. Bond, Acta Cryst. 13 (1960) 814.
[16] G.R. Jones, I.M. Young and R.F.C. Farrow, to be published.
[17] J. Hornstra and W.J. Bartels, J. Crystal Growth 44 (1978) 513.
[18] J.D.H. Donnay and H.M. Ondik, Crystal Data – Determinative Tables, Vol. 2, Inorganic Compounds, 3rd ed. (NSRDS/JCPDS, USA, 1973) p. C-162.
[19] Ref. [18], p. C-123.
[20] A.W. Ewald, J. Appl. Phys. 25 (1954) 1436.
[21] O.N. Tufte and A.W. Ewald, Phys. Rev. 122 (1961) 1431.
[22] National Bureau Standards (US) Tech. Note 270-3 (NBS, Washington, DC, 1978).
[23] J.H. van der Merwe, Critical Rev. Solid State Sci. Mater Sci. 7 (1978) 209.
[24] V. Montgomery, A. McKinley and R.H. Williams, Surface Sci. 89 (1979) 635.
[25] S.H. Groves and W. Paul, Phys. Rev. Letters 11 (1963) 194.
[26] M. Averous, Phys. Status Solidi (b) 95 (1979) 9.
[27] S.I. Novikova, in: Semiconductors and Semimetals, Vol. 2, Eds. R.K. Willardson and A.C. Beer (Academic Press, New York, 1966) ch. 2.
[28] A.N. Nesmeyanov, Vapour Pressure of the Elements (Infosearch, London, 1963).